Rare Metal Materials and Engineering
Volume 49, Issue 6, June 2020
Available online at www.rmme.ac.cn

Science Press

Cite this article as: Rare Metal Materials and Engineering, 2020, 49(6): 1915-1924.

ARTICLE

Influence of Yb and Al-Ti-B Complex Modification on Microstructure and Performance of Hypereutectic Al-Si Casting Alloys

Li Qinglin, Zhu Yuqian, Li Jinbao, Li Binqiang, Liu Jianjun, Liu Dexue, Lan Ye-feng, Xia Tiandong

State Key Laboratory of Advanced Processing and Recycling of Non-ferrous Metal, Lanzhou University of Technology, Lanzhou 730050, China

Abstract: The microstructure evolution and mechanical properties of hypereutectic Al-20Si alloy containing rare earth Yb and Al-5Ti-1B refiner were investigated. The microstructures of the samples were characterized by optical microscopy, scanning electron microscopy, and electron probe microanalysis. Microstructural analysis demonstrates that the primary Si is significantly refined from a coarse polygonal, platelet-like or star-like shape into a fine blocky shape; the eutectic Si structure is modified from a coarse platelet-like/needle-like structure into fine particles or a fibrous structure; and the coarse α-Al dendrites are refined into fine equiaxed dendrites after addition mass fraction of 0.5% Yb and 0.3% Al-5Ti-1B complex. However, the primary and eutectic Si phases become coarser when the content of Al-5Ti-1B refiner reaches 0.4%. The mechanical properties of the Al-20Si alloy with different modifiers and different modifier concentrations were investigated by the tensile test. The results show that after combined addition of 0.5% Yb and 0.3% Al-5Ti-B the ultimate tensile strength and elongation of the prepared sample increase by 83.7% and 92.1%, respectively.

Key words: hypereutectic Al-20Si alloy; primary Si; eutectic Si; rare earth Yb; Al-5Ti-1B refiner; mechanical properties

With high fluidity, good wear and corrosion resistance, good thermal conductivity, low thermal expansion coefficient, and high strength to weight ratio, aluminum-silicon (Al-Si) alloys have been extensively employed in aerospace, automotive, and general engineering industries[1-5]. Recently, with increasing demand for light vehicles featuring improved fuel efficiency and reduced greenhouse gas emissions, hypereutectic Al-Si alloys have been widely recognized as attractive candidate materials for automotive piston manufacturing owing to them being lightweight and having good wear resistance[6,7]. It is well known that hypereutectic Al-Si alloys consist of primary Si phases, α-Al, and eutectic Si. Si is a faceted phase; therefore, the primary Si phases are usually of a coarse, irregular star-like (five-folded), plate-like, or polygonal morphology, whereas the eutectic Si phases normally grow into coarse acicular/flake morphology during the conventional casting process of hypereutectic Al-Si alloys. Previous studies have shown that the size, morphology, and distribution of primary and eutectic Si phases play an important role in determining the mechanical properties and wear behaviors of hypereutectic Al-Si alloys[8,9]. The coarse primary Si and acicular Si act as premature crack initiators that lead to weakened mechanical properties and inferior sliding wear [10]. Thus, uniformly-distributed primary Si and fine eutectic Si phases need to be formed to improve the mechanical and tribological properties of hypereutectic Al-Si alloys.

Considerable efforts have been made to modify the primary and eutectic Si phases in hypereutectic Al-Si alloys. Refinement of Si phases can be achieved by different techniques such as chemical modification[11], melt superheating treat-

Received date: June 21, 2019
Foundation item: National Natural Science Foundation of China (51561021)
Corresponding authors: Li Qinglin, Ph. D., Associate Professor, School of Materials Science and Engineering, Lanzhou University of Technology, Lanzhou 730050, P. R. China, Tel: 0086-931-2976688, E-mail: liql301@mail.nwpu.edu.cn

ment[12], outfield treatment[13], rapid solidification[14], and spray forming[15]. Chemical modification via the addition of modifiers or nucleation agents has been widely used during the conventional casting process of Al-Si alloys because of its high effectiveness and simplicity. Elemental strontium and sodium have gained popularity as efficient modifiers in the modification of hypereutectic and eutectic Al-Si alloys[16,17], and can change the morphology of eutectic Si from a coarse needle-like/flake-like structure to a fine coral fibrous structure. In addition, it has been reported in published literature[18-20] that the primary Si crystals could be effectively refined after red phosphorous, phosphate salt, Al-P, or Cu-P master alloy were added to the hypereutectic Al-Si alloy melt. Researchers believe that AlP particles could act as the heterogeneous nuclei of primary Si crystals during solidification due to their similar crystal structure and lattice parameters to Si[21]. Moreover, Zuo et al[22] found that the combined addition of P and Sr could simultaneously refine and modify primary and eutectic Si of hypereutectic Al-30Si alloy at a melting temperature of 770 °C.

Recently, the effects of rare earth elements on the morphology and size of Si phases of Al-Si alloys have been investigated. The author found that rare earth Ce or Er had a good modification effect on primary and eutectic Si phases and improved the mechanical properties of the hypereutectic Al-20Si alloy. Chang et al[23,24] showed that mischmetal could simultaneously refine the primary and eutectic Si phases of hypereutectic Al-21%Si alloy. Fatih Kilicaslan et al[25] stated that Sc refined the size of the primary and eutectic Si of Al-20Si alloy, but did not significantly change their morphologies. In addition, rare earth elements can effectively modify eutectic Si in Al-Si alloys, such as Yb[25], La[26], Eu[27], Gd[28], and Sm[29]. Yu et al[30] reported that the coupling of AlP and Al_4C_3 particles could remarkably improve the modification efficiency of primary Si. Prasada Rao et al[31] reported that the combined addition of Al-Ti-C and Sr significantly refined the α-Al and eutectic Si structure in the Al-7Si-0.3Mg alloy. Liao et al[32] stated that the combined addition of strontium and boron led to a much greater decrease in the eutectic grain size of near-eutectic Al-Si alloys compared with that caused by the addition of strontium alone. Furthermore, the addition of Al-P-Ti-TiC-Nd refiner not only modified eutectic Si but also refined primary Si in hypereutectic Al-20Si alloy, and achieved a much finer size of Si phases compared with the addition of Al-P-Ti-TiC refiner[33]. Recently, Liu et al[34] showed that the separate addition of Gd or Zr had almost no effect on the modification of eutectic Si, whereas the combined addition of Gd and Zr significantly refined the eutectic Si and changed its morphology. Thus, the combined addition of modifiers has a much better modification effect than the separate addition of modifiers.

Previous studies have discussed the effect of rare earth Yb or Al-Ti-B/Al-Ti-C master alloy on eutectic Si and α-Al in Al-Si casting alloys. However, the synergistic effect of Yb and Al-Ti-B on the microstructure and mechanical properties in hypereutectic Al-Si alloy has not been reported to date. In the present study, the effects of Yb and Al-Ti-B complex modification on the microstructure and mechanical properties of Al-20Si alloy were investigated, and the mechanism of modification was discussed.

1 Experiment

Commercial hypereutectic Al-20%Si (all percentages are wt% unless otherwise stated) alloy was melted in a clay-bonded graphite crucible in an electrical resistance furnace at 750 °C for 30 min. First, 0.5% Yb was added to the melt, wrapped in aluminum foil, and stirred for 10 min to ensure homogeneity of composition. Next, various contents of Al-5Ti-1B master alloys were added to the Al-20Si-0.5Yb alloy melt, with a nominal addition mass fraction of 0.1%, 0.2%, 0.3% and 0.4%. Finally, the melting was degassed using a commercial degasser of solid hexachloroethane (C_2Cl_6). After the melt slag was skimmed, the melt was poured into a 200 °C preheated permanent steel mold (20 mm inner diameter and 100 mm length) and heated to 720 °C. The samples were prepared according to standard metallographic procedures and then etched using Keller's reagent (2.5 mL HNO_3, 1.5 mL HCl, 1 mL HF, and 95 mL H_2O). The microstructures of the samples were characterized using scanning electron microscopy (SEM), optical microscopy, and electron probe microanalysis (EPMA). Image Pro-Plus software was used to measure the average size of the primary Si crystals. To reveal the three-dimensional (3D) morphology of the eutectic Si structure, Si particles were extracted from the solidified samples with the different modifiers. Tensile specimens were machined according to the GB/T228-2002 standard with dimensions of 25 mm in length and 5 mm in diameter. The mechanical properties of the Al-20Si alloy with the separate addition of a modifier or the combined addition of multiple modifiers were measured at room temperature (25~30 °C) with the material test system (AG-10TA). The fracture surfaces of the tensile specimens were also examined by SEM to evaluate the fracture mechanism.

2 Results and Discussion

2.1 Analysis of microstructure

The influence of Yb and Al-5Ti-1B complex modification on the microstructural evolution of hypereutectic Al-20Si alloy was investigated. Micrographs in Fig.1 show the morphology and size of the primary and eutectic Si of the unmodified Al-20Si alloy. Fig.1a shows that the morphology of the primary Si phase is a coarse and irregular platelet, polygon or star-like shape, and the average size is approximately 158 μm. As illustrated in Fig.1b, the eutectic Si crystals are distributed in the metal matrix in the form of coarse needles/platelets. Fig.2 indicates the microstructure of

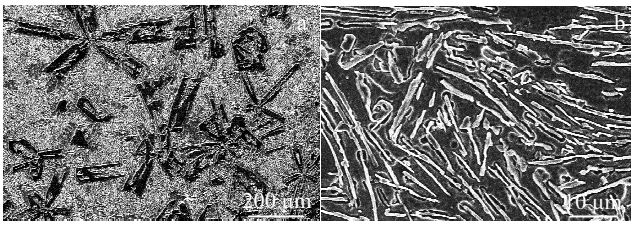

Fig.1 Micrographs of unmodified hypereutectic Al-20Si alloy: (a) primary Si and (b) eutectic Si

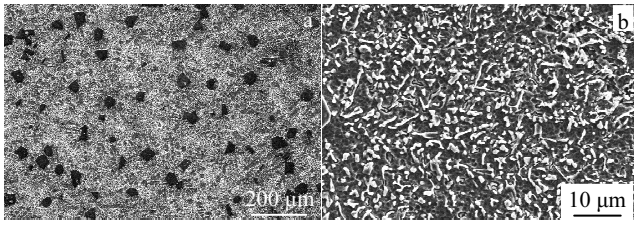

Fig.2 SEM micrographs of hypereutectic Al-20Si alloy modified with 0.5% Yb: (a) primary Si and (b) eutectic Si

Al-20Si modified with 0.5% Yb. Compared with the unmodified samples, the coarse star-shaped and plate-like primary Si is refined into a fine blocky shape, and the average size of the primary Si decreases to 47 μm, as shown in Fig.2a. Moreover, Fig.2b clearly shows that the size of the eutectic Si drastically decreases and the morphology of the eutectic Si is modified into fine branched and granular structures. Fig.3 shows the microstructures of the primary Si phases of the Al-20Si alloys modified with the Al-5Ti-1B master alloy (the addition content is 0.1%, 0.2%, 0.3%, and 0.4%). As shown in Fig.3a~3d, the morphologies of the primary Si phases do not significantly change, which is different from what was observed in the unmodified alloy (Fig.1a); the mean size of the primary Si decreases from 158 μm to 97 μm as the addition amount of Al-5Ti-1B increases from 0.1% to 0.3%. However, the size of the primary Si becomes coarser when the addition amount of the Al-5Ti-1B refiner reaches 0.4%. Fig.4 shows the microstructures of the eutectic Si phase of Al-20Si alloys modified with 0.1%, 0.2%, 0.3% and 0.4% Al-5Ti-1B. The size and interflake spacing of the eutectic Si remarkably decrease with the increase in addition amount. However, the morphology of the eutectic Si structure is still lamellar, as shown in Fig.4a~4d. Moreover, the eutectic Si structure does not further change when the addition content of Al-5Ti-1B reaches 0.4%.

To investigate the effect of Yb and Al-5Ti-1B complex modification on the morphology and size of primary and eutectic Si phases, different concentrations (0.1%, 0.2%, 0.3%, and 0.4%) of Al-5Ti-1B were added to the Al-20Si alloy containing 0.5% Yb. The SEM images of the primary Si phases modified with the different contents of Al-5Ti-1B refiner are shown in Fig.5. Comparing the size and distribution of the primary Si phases with combined addition and separate addition of 0.5% Yb (Fig.2a), it is found the complex modification of Yb and Al-5Ti-1B has a greater effect on the size and distribution of the primary Si phases (Fig.5). Primary Si phases are effectively refined and homogeneously distributed in the (α-Al+Si) eutectic matrix as the addition content of the Al-5Ti-1B refiner increases from 0.1% to 0.3% (Fig.5a~5c). However, the primary Si crystals do not further refine when the addition concentration of Al-5Ti-1B reaches 0.4% (Fig.5d). Fig.5e shows the 3D morphology of the primary Si particles extracted from the Al-20Si alloy containing 0.5% Yb and 0.3% Al-5Ti-1B. The primary Si particles are shown to be of a regular octahedron shape and no significant hollows appear on the surface of the Si particles (Fig.5e). Fig.6 shows the

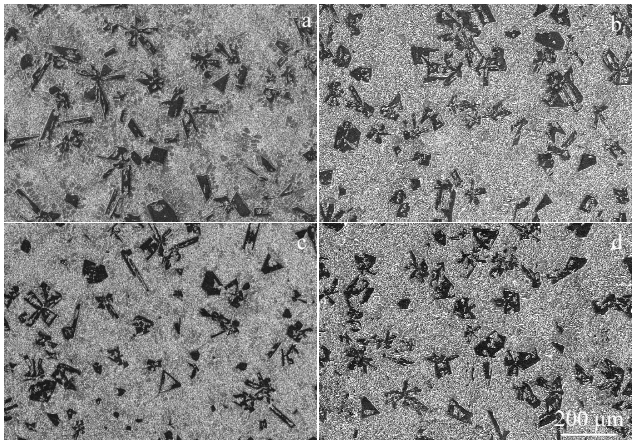

Fig.3 SEM micrographs of the primary Si phases of hypereutectic Al-20Si alloy modified with 0.1% Al-5Ti-1B (a), 0.2% Al-5Ti-1B (b), 0.3% Al-5Ti-1B (c), and 0.4% Al-5Ti-1B (d)

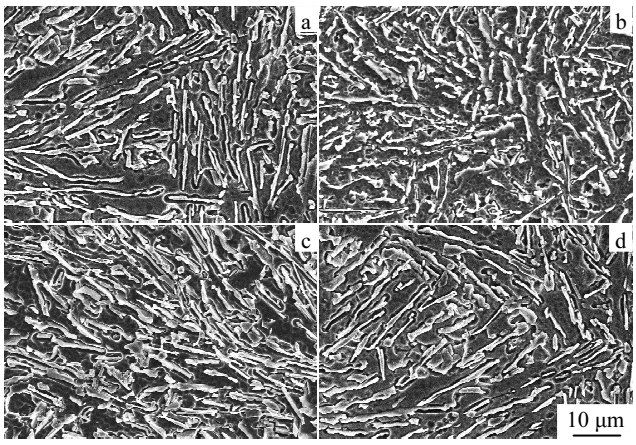

Fig.4 Eutectic Si structural characteristics of Al-20Si alloy modified with 0.1% Al-5Ti-1B (a), 0.2% Al-5Ti-1B (b), 0.3% Al-5Ti-1B (c), and 0.4% Al-5Ti-1B (d)

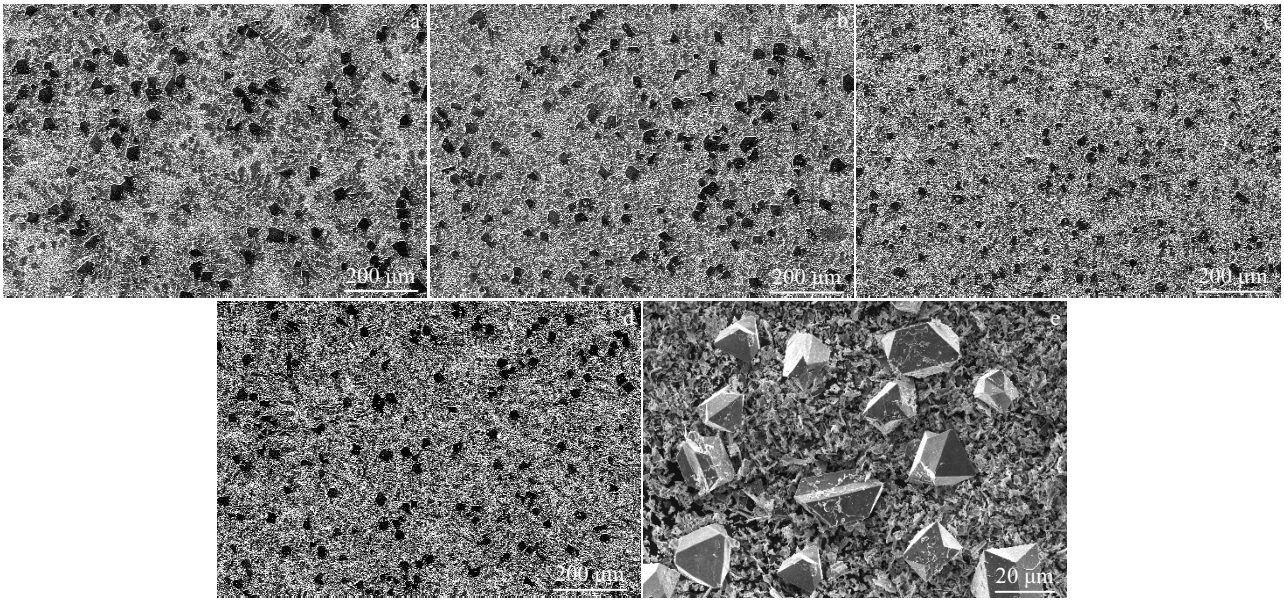

Fig.5 SEM images of the primary Si phases of hypereutectic Al-20Si-0.5Yb modified with 0.1% Al-5Ti-1B (a), 0.2% Al-5Ti-1B (b), 0.3% Al-5Ti-1B (c) and 0.4% Al-5Ti-1B (d); 3D morphology of primary Si particles extracted from Fig.5c (e)

modification effect of Al-5Ti-1B on the mean size of the primary Si of the Al-20Si-0.5Yb alloy. The average size of the primary Si phase gradually decreases from 47 μm to 28 μm with the increasing content of the Al-5Ti-1B refiner from 0.1% to 0.3%. When the content of the Al-5Ti-1B increases to 0.4%, the average size of the primary Si particles increases to 34 μm, which is still smaller than that of the Al-20Si-0.5Yb alloy modified with 0.2% Al-5Ti-1B (Fig.6).

The effect of Yb and Al-5Ti-1B complex modification on the eutectic Si structure is shown in Fig.7. By comparing Fig.2b with Fig.7a~7c, it can be observed that the complex modification treatment has a more significant effect on the eutectic Si structure than the modification effect by the separate addition of the Yb or Al-5Ti-1B master alloy. The size of the eutectic Si structure of the Al-20Si-0.5Yb alloy dramatically decreases with the increase of the addition content of the Al-5Ti-1B refiner. Moreover, the morphology of the eutectic Si is mainly present in the form of fine particles and fiber (Fig.7a~7c). By comparing Fig.7c with Fig.7d, no significant change appears in the size and morphology of the eutectic Si structure when the addition content of Al-5Ti-1B refiner reaches 0.4%, but it rather remains in granular and fibrous form. This result is in agreement with the above discussions on the refinement of the primary Si phases. A higher level than optimum content results in an over-modified structure characterized by a coarse microstructure. A previous study showed that the addition quantity of modifiers or refiners beyond a certain level would no longer lead to further structural refinement although more nucleation agents would be provided[35]. This is because releasing latent heat produces recalescence, thus leading to less undercooling. In addition, the aggregation probability of nucleation particles might increase with the addition amount of the inoculants. To further investigate the morphological evolution, SEM characterization was performed to characterize the 3D morphology of the eutectic Si structure extracted from the Al-20Si alloy containing 0.5% Yb and various contents of Al-5Ti-1B (Fig.8). The morphology of eutectic Si changes from a coarse platelet-like to a fine coral-like fibrous structure and the size remarkably decreases with the increase of the addition amount of the Al-5Ti-1B refiner.

To explain the formation mechanism of the coarse Si crystals and the modification mechanism of the Si crystals, the twin plane re-entrant angle edge (TPRE) mechanism and the impurity induced twinning (IIT) mechanism were proposed.

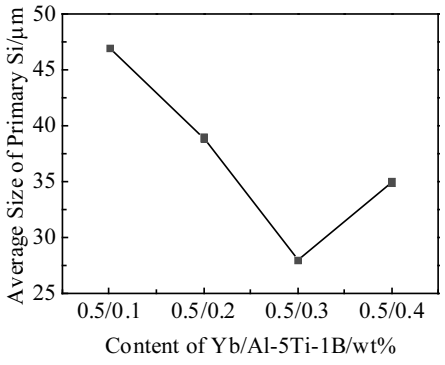

Fig.6 Average size of the primary Si in the Al-20Si-0.5Yb alloy after combined addition of Yb and Al-5Ti-1B

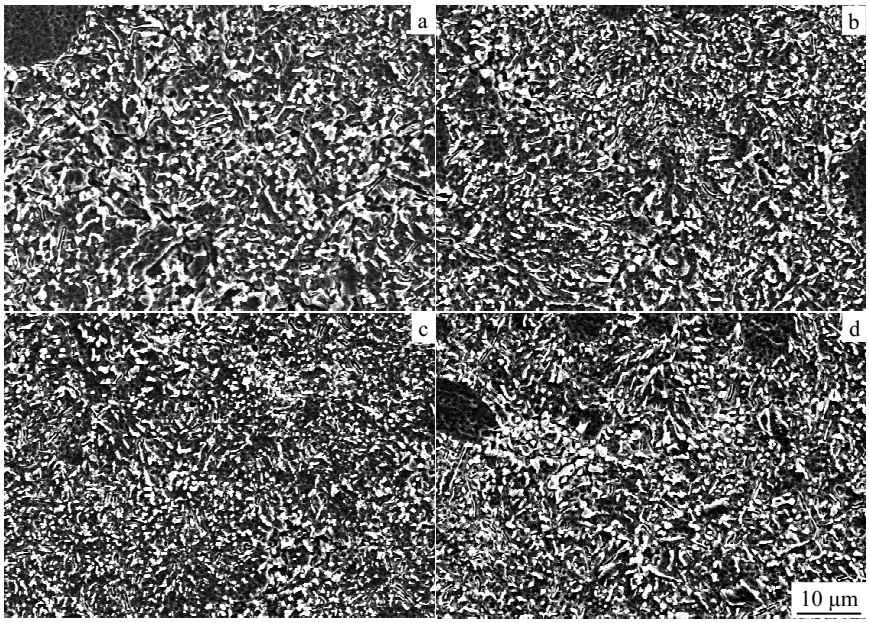

Fig.7 SEM micrographs of the eutectic Si of hypereutectic Al-20Si-0.5Yb alloy modified with 0.1% Al-5Ti-1B (a), 0.2% Al-5Ti-1B (b), 0.3% Al-5Ti-1B (c), and 0.4% Al-5Ti-1B (d)

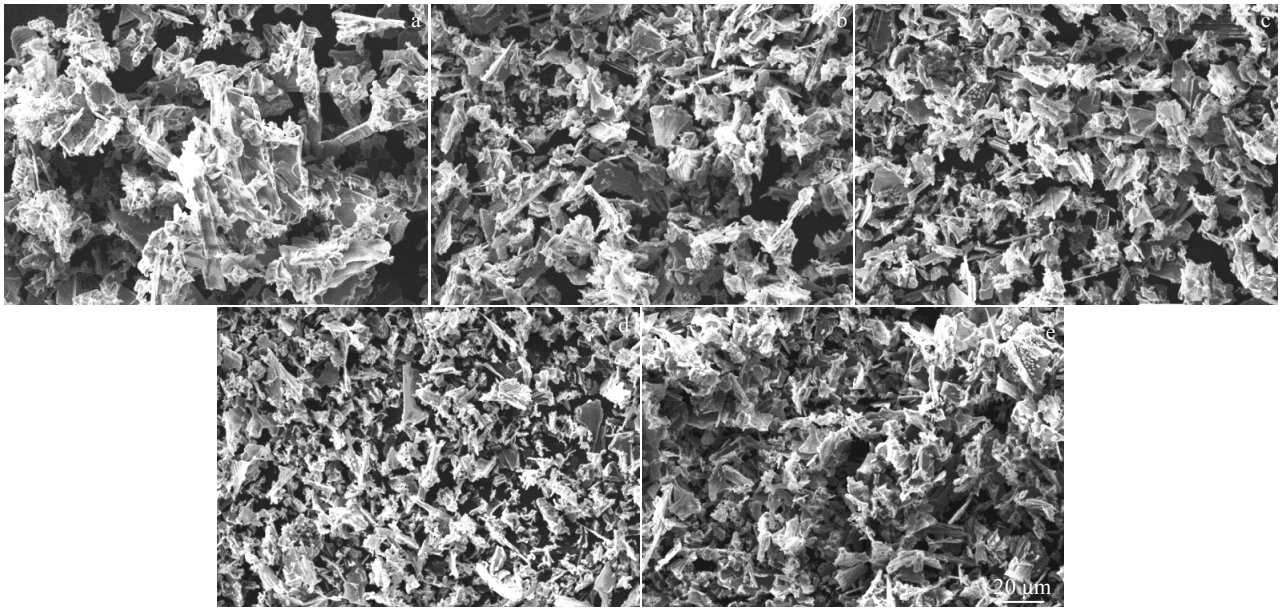

Fig.8 3D morphologies of eutectic Si structure of Al-20Si alloy after the combined addition of Yb and Al-5Ti-1B: (a) without any addition, (b) with addition of 0.5% Yb+0.1% Al-5Ti-1B, (c) with addition of 0.5% Yb+0.2% Al-5Ti-1B, (d) with addition of 0.5% Yb+0.3% Al-5Ti-1B, and (e) with addition of 0.5% Yb+0.4% Al-5Ti-1B

According to the TPRE mechanism, Si growth occurs more readily at the re-entrant edge along the <112>Si growth direction of Si[36]. According to the IIT mechanism, the atoms of the modifier are absorbed on the growing $\{111\}_{Si}$ steps, which causes frequent multiple Si twins. The mechanism indicates that the atoms of the modifier are absorbed into the growth steps of the Si solid-liquid interface, which alters the Si growth mode from facet growth to non-facet growth, resulting in the refinement of Si crystals. Lu and Hellawell[37] proposed that a growth twin would be created at the interface

when there was an ideal ratio between the atomic radius of the adsorption elements and the radius of silicon close to 1.646. The result shows that the elements of modification are more easily absorbed at ledges on the growing $\{111\}_{Si}$ surface changing the stacking sequence when the atomic radius ration is close to 1.65. The atomic radius of Yb is 0.24 nm and that of Si element is 0.146 nm; therefore, the r_{Yb}/r_{Si} ratio is 1.644, which is very close to the ideal ratio of 1.646. As well known, rare earth Yb is one type of surface active elements. The atoms of Yb can be absorbed onto growth front and effectively poison the growth steps inducing the higher twin density, which results in the isotropic growth of eutectic Si during the solidification. However, it has been reported that the atomic radius ration is not only a universal law that the elements can induce frequent twinning[24,38].

Fig.9 shows the optical micrographs of hypereutectic Al-20Si alloy modified with 0.5% Yb and various concentrations of Al-5Ti-1B refiner. The α-Al phases are the typical dendrites. It can be seen from circles in Fig.9a that the α-Al phases in the unmodified Al-20Si alloy are coarse dendrites, and the size is about 600 μm. In addition, it is difficult to differentiate grain boundary of α-Al dendrites and there is no apparent the secondary dendrite arm (SDA). However, the boundaries between the α-Al dendrites and eutectic Si are clear and the size of the α-Al dendrites significantly decrease when 0.5% Yb is added to the Al-20Si alloy (Fig.9b). Fig.9c~9e show a significant refinement of α-Al dendrites in the Al-20Si-0.5Yb alloy as the addition content of Al-5Ti-1B increases from 0.1% to 0.4%. The coarse α-Al dendrites turn into fine equiaxed dendrites in the red circles of Fig.9e, and the size is about 100 μm. Besides, the secondary dendrite arm spacing (SDAS) significantly decreases with the increasing of addition concentration of Al-5Ti-1B master alloy, as shown in Fig.9. The result shows that the Al-5Ti-1B refiner can not only effectively refine wrought aluminum alloys, but also significantly refine the α-Al dendrites of the Al-20Si alloy.

Fig.10 shows the typical results of the EPMA analysis of the Al-20Si-0.5Yb alloy with the addition of 0.3% Al-5Ti-1B refiner. The compositional distribution is illustrated by the X-ray mapping of elements Al, Si, Yb, Ti, and B of the Al-20Si alloy with the combined addition of Yb and Al-5Ti-1B. Fig.11 shows the element distribution along line A-B. During the solidification process, part of Yb is rejected to the front of the advancing solid-liquid interface and the Yb-containing phase forms because Yb has a very limited solubility in Al and Si. Fig.10 and Fig.11a show that the Yb-contained phase consists of elements Al, Yb, and Si. Li et al[39] observed the formation of the Al_2Si_2Yb phase when 0.1% Yb was added to the Al-5Si alloy, which resulted in an intensive constitutional undercooling in the front of the solid-liquid interface. In addition, the previous literature[24] has pointed that the undercooling increases because of reduction of nucleation with increasing the Yb concentration in Al-7Si alloy. Hence, the Si phases could be significantly refined due to restricting the growth of the Si phases. A minor addition of Ti (0.3% Al-5Ti-1B) could lead to the formation of AlTiSi particles distributed in the core of the primary Si and in α-Al matrix (Fig.10 and Fig.11b). Moreover, Ghomashchi[40]

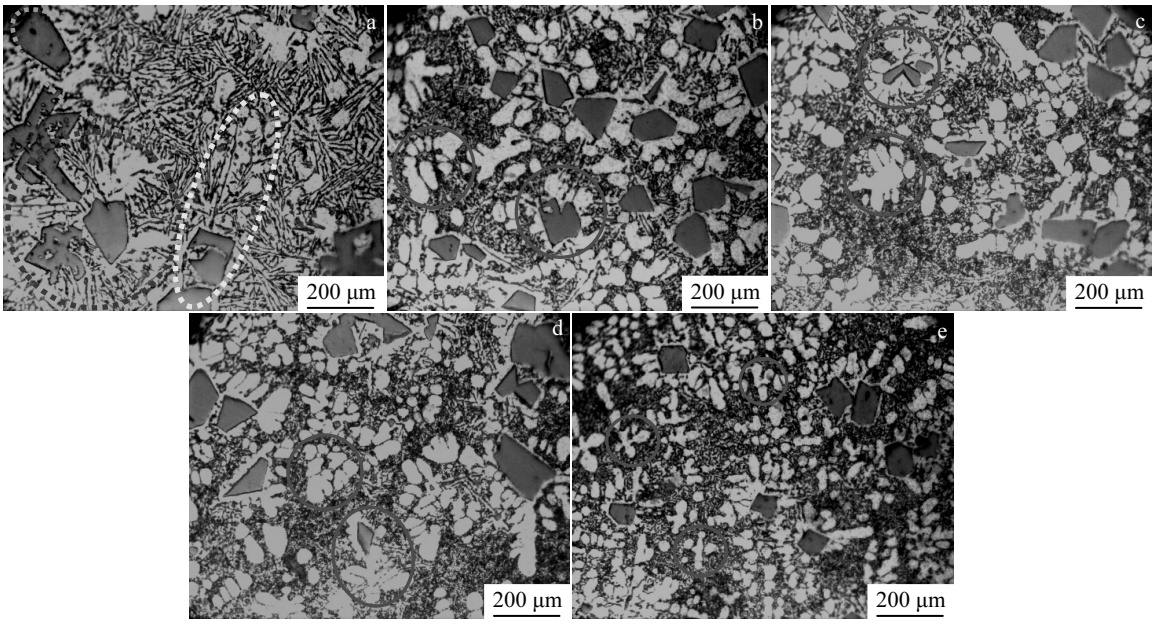

Fig.9 Optical micrographs of hypereutectic Al-20%Si alloy after the combined addition of Yb and Al-5Ti-1B: (a) without any addition, (b) with addition of 0.5% Yb+0.1% Al-5Ti-1B, (c) with addition of 0.5% Yb+0.2% Al-5Ti-1B, (d) with addition of 0.5% Yb+0.3% Al-5Ti-1B, and (e) with addition of 0.5% Yb+0.4% Al-5Ti-1B

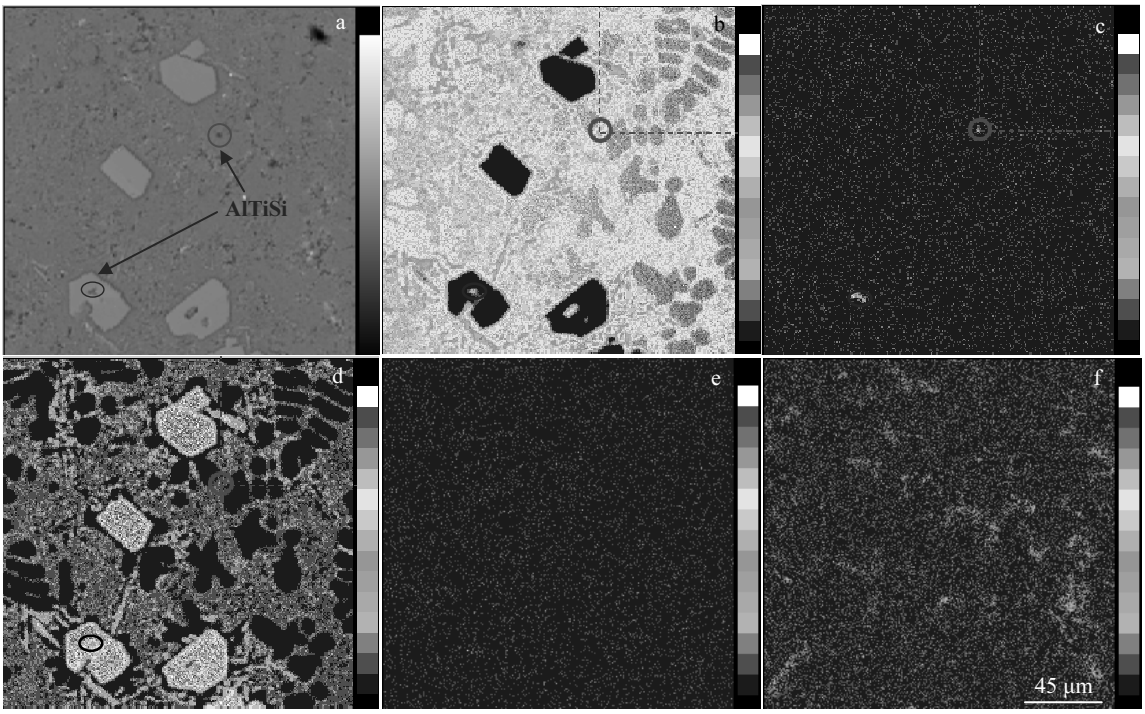

Fig.10 Backscattered electron image (a) and mapping analysis of Al-20Si-0.5Yb alloy with the addition of 0.3% Al-5Ti-1B by EPMA: (b) Al, (c) Ti, (d) Si, (e) B, and (f) Yb

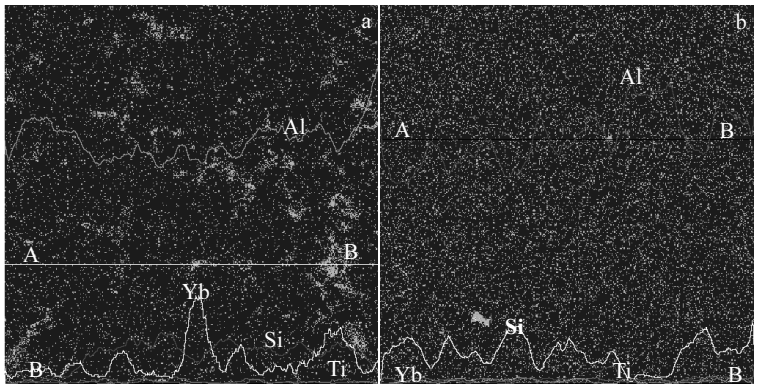

Fig.11 Line scanning of elements along the A-B line in Yb and Ti mapping image: (a) across Yb-containing particles and (b) across Ti-containing particle

reported that Ti-added A356 alloy formed AlTiSi particles, particularly when the Ti concentration was less than 0.15%, and presented two possible orientation relationships between AlTiSi particles and Al, as shown below:

(002)Al//(020)AlTiSi, [001]Al//[010]AlTiSi

(111)Al//(211)AlTiSi, [111]Al//[112]AlTiSi

Wang et al[41] reported Al-5Ti-1B master alloy is the most widely-used grain refiner for wrought Al alloys, since it can react with Al to form $TiAl_3$ and TiB_2 particles which can act as heterogeneous nucleation sites of α-Al. However, it is failed to refine Al-Si casting alloys when the Si content is higher than 5%. This is because Si tends to react with Ti to form Ti-rich silicides, such as $TiSi_2$ or TiAlSi phases[42]. According to Ref. [33], the precipitation of complex Ti-Al-Si intermetallic may be adsorbed upon the growth steps of silicon crystal and furthermore prevent the growth of primary silicon. Moreover, it has been obviously found that the precipitation Ti-rich (AlTiSi) particle is surrounded in the core of primary Si in the Al-20Si alloy, as shown in Fig.11b. The result shows that the fine AlTiSi particle can act as potential nucleating site. On the other hand, the amount of AlTiSi particles may decrease since the forming is restricted after the combined addition of rare earth Yb and Al-5Ti-1B master alloy. Hence, the combined addition of modifiers has a much better modification effect on the

microstructure including α-Al, eutectic Si and primary Si phases.

2.2 Analyses of mechanical properties

Fig.12 shows the typical ultimate tensile strength (UTS) and elongation (El) of the unmodified Al-20Si alloy, Al-20Si alloy with separate addition of 0.3% Al-5Ti-1B or 0.5% Yb, as well as Al-20Si alloys with the combined addition of Yb and Al-5Ti-1B. The separate addition of Yb, the combined addition of Yb and Al-5Ti-1B both significantly improve the mechanical properties of all tested samples (Fig.12). The UTS of Al-20Si alloy, Al-20Si-0.3(Al-5Ti-1B) alloy, Al-20Si-0.5Yb alloy, Al-20Si-0.5Yb-0.1(Al-5Ti-1B) alloy, Al-20Si-0.5Yb-0.2(Al-5Ti-1B) alloy, Al-20Si-0.5Yb-0.3(Al-5Ti-1B) and Al-20Si- 0.5Yb-0.4(Al-5Ti-1B) alloy are 92, 109, 151, 154, 162, 169, and 166 MPa, respectively. The El of the alloys are 0.38%, 0.42%, 0.66%, 0.69%, 0.71%, 0.73% and 0.72%, respectively. The UTS enhances by 83.7% from 92 MPa to 169 MPa, and El increases by 92.1% from 0.38% to 0.73% after the combined addition of 0.5% Yb and 0.3% Al-5Ti-1B. The Al-20Si alloy modified with 0.5% Yb and 0.3% Al-5Ti-1B has the largest UTS and El. These results are consistent with the microstructural evolution mentioned previously. It is well known that the mechanical properties of hypereutectic Al-20Si alloy mainly depend on the morphology, size, and distribution of primary and eutectic Si crystals. Hence, both UTS and El can be significantly improved when primary and eutectic Si phases are refined or modified by Yb and Al-5Ti-1B complex modification. This is because the fine primary and eutectic Si can eliminate the initiation of premature cracks in tension environments.

Fig.13 shows the fracture surfaces of the various modified

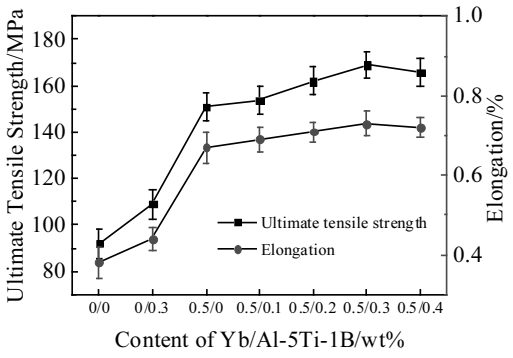

Fig.12 Mechanical properties of hypereutectic Al-20Si alloy with different modifications

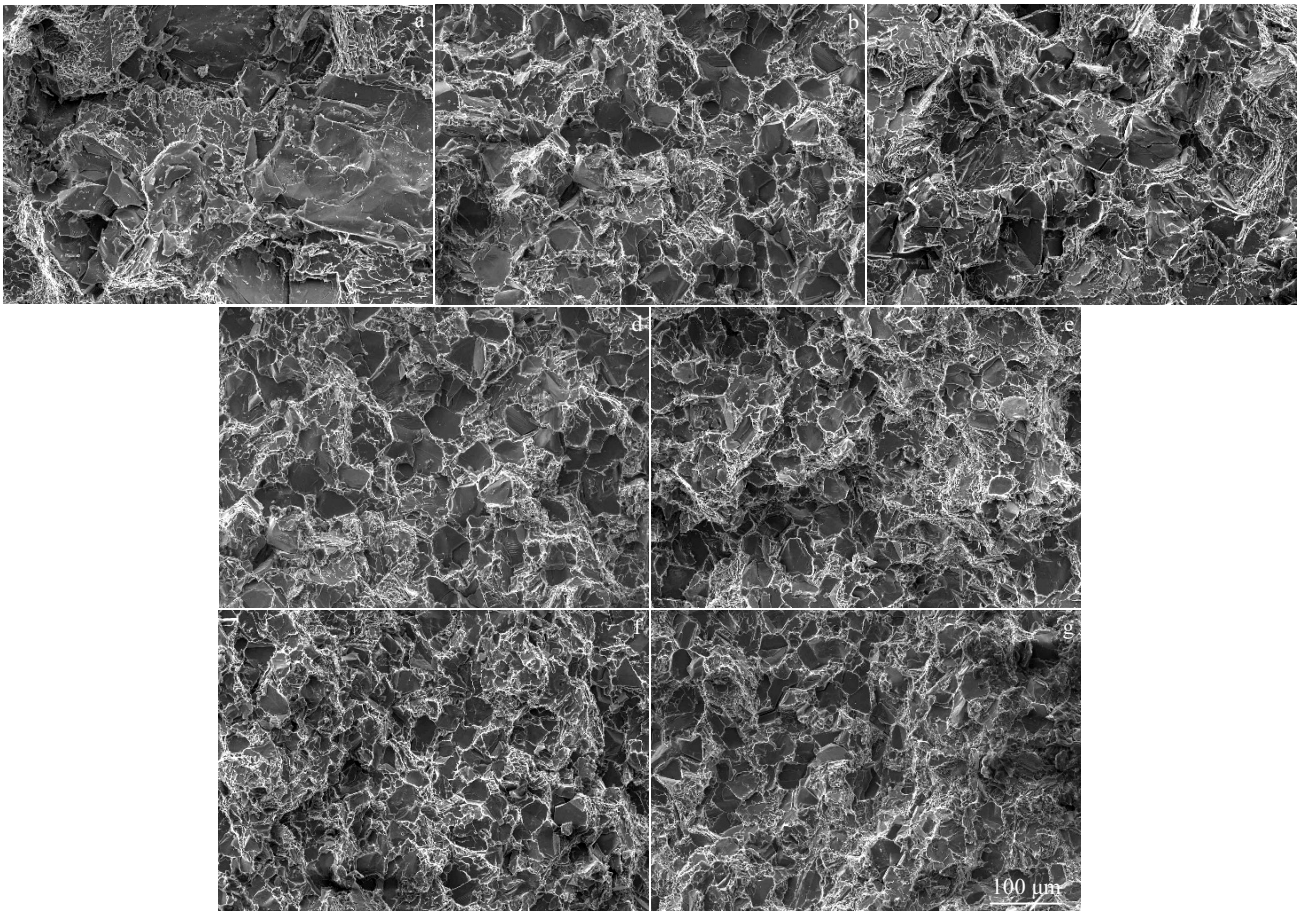

Fig.13 Fractographs of the tensile samples of hypereutectic Al-20Si alloy with different modifications: (a) without inoculation, (b) 0.3% Al-5Ti-1B, (c) 0.5% Yb, (d) 0.5% Yb+0.1% Al-5Ti-1B, (e) 0.5% Yb+0.2% Al-5Ti-1B, (f) 0.5% Yb+0.3% Al-5Ti-1B, and (g) 0.5% Yb+0.4% Al-5Ti-1B

alloys after tensile testing. For unmodified alloy and alloy modified with separate addition of 0.5% Yb or 0.3% Al-5Ti-1B, the fracture surfaces are completely covered by cleavage plane (Fig.13a~13c). The fracture surface shows typical brittle fracture as intergranular failure is caused by the coarse primary Si phases. In addition, the fracture surfaces are composed of smaller cleavage planes and tearing ridges as rare earth Yb and Al-5Ti-1B are simultaneously added into the Al-20Si alloy (Fig.13d~13g). It has been reported that the fracture mechanism of Al-Si alloys is mainly attributed to three factors [43]: (a) the size and distribution of the silicon crystals, (b) the bonding strength between the silicon crystals and the matrix and (c) the ease with which the Si crystals crack. Griffith equation[44] gives the relation between the intrinsic fracture stress (σ_f) on the primary silicon and the internal defects length (C):

$$\sigma_f = \left(\frac{2E\gamma}{\pi C}\right)^{\frac{1}{2}} \quad (1)$$

where γ is the fracture surface energy; E is the Young's modules of the particles. According to the Griffith equation, the internal defects of coarse primary Si crystals are much longer than those of fine Si crystals, which lowers the intrinsic fracture stress (σ_f). On the other hand, coarse irregular primary Si and flake-like eutectic Si present sharp edges or ends, which are stress concentration sites and preferred cracks initiation. Therefore, refinement of primary Si crystals and modification of eutectic Si structure can evidently enhance tensile strength. In addition, according to classical Hall-Petch equation[45]:

$$\sigma_s=\sigma_0+kd^{-0.5} \quad (2)$$

where σ_0 represents the grain interior resistant to deformation, k is the strengthening coefficient and d is the diameter of the grain. The equation shows the finer the size of α-Al grains is, the higher the strength and ductility is. Hence, the combined effect of modifying Si phases and refining α-Al dendrites is more beneficial to enhancement of mechanical properties (UTS and El) than in unmodified Al-20Si alloy.

3 Conclusions

1) The separate addition of 0.5% Yb effectively modifies the primary and eutectic Si crystals. However, the separate addition of Al-5Ti-1B only decreases the size of the primary and eutectic Si, rather than changing the morphology of the Si phases.

2) The combined addition of 0.5% Yb and Al-5Ti-1B significantly refines the primary Si crystals, making the morphology of Si crystals change into fine block, the morphology of eutectic Si phases changes into fine particles and fibrous structure when the addition of Al-5Ti-1B reaches 0.3%.

3) The combined addition of 0.5% Yb and Al-5Ti-1B can significantly refine the α-Al dendrites from coarse dendrites to small equiaxed dendrites.

4) The UTS and El significantly improve owing to the refinement and modification of Si crystals and α-Al dendrites. After combined addition of 0.5% Yb and 0.3% Al-5Ti-1B, the UTS increases by 83.7% and the El increases by 92.1%.

References

1 Haghshenas M, Jamali J. *Case Studies in Engineering Failure Analysis*[J], 2017, 8: 11

2 Yu W H, Zhang Y, Yan T L *et al*. *Journal of Alloys and Compounds*[J], 2017, 693: 303

3 Lu D H, Jiang Y H, Guan G S *et al. Journal of Materials Processing Technology*[J], 2007, 189: 13

4 Hekmat-Ardakan A, Ajersc F. *Acta Materialia*[J], 2010, 58: 3422

5 Rajua K, Harsha A P, Ojha S N. *Materials Science and Engineering A*[J], 2011, 528: 7723

6 Bolzoni L, Hari Babu N. *Applied Materials Today*[J], 2016, 5: 255

7 Chen M, Alpas A T. *Wear*[J], 2008, 265: 186

8 Xu C, Xiao W L, Zheng R X *et al. Materials & Design*[J], 2015, 88: 485

9 Joy Yii S L, Anas N M, Ramdziah M N *et al. Procedia Chemistry*[J], 2016, 19: 304

10 Elmadagli M, Perry T, Alpas A T. *Wear* [J], 2007, 262: 79

11 Liu X F, Wu Y Y, Bian X F. *Journal of Alloys and Compounds*[J], 2005, 391: 90

12 Li Q L, Xia T D, Lan Y F *et al. Materials Science and Technology*[J], 2014, 30: 835

13 Feng H K, Yu S R, Li Y L *et al. Journal of Materials Processing Technology* [J], 2008, 208: 330

14 Cai Z Y, Wang R C, Zhang C *et al. Advanced Powder Technology*[J], 2015, 26: 1458

15 Cui C, Schulz A, Schimanski K *et al. Journal of Materials Processing Technology*[J], 2009, 209: 5220

16 Lu L, Nogita K, Dahle A K. *Materials Science and Engineering A* [J], 2005, 399: 244

17 Dahle A K, Nogita K, McDonald S D *et al. Materials Science and Engineering A* [J], 2005, 413: 243

18 Zhang H H, Duan H L, Shao G J *et al. Rare Metals*[J], 2008, 27: 59

19 Wu Y P, Wang S J, Li H *et al. Journal of Alloys and Compounds*[J], 2009, 477: 139

20 Liu X F, Wu Y Y, Bian X F. *Journal of Alloys and Compounds*[J], 2005, 391: 90

21 Bao G J, Zuo M, Li D K *et al. Materials Science and Engineering A* [J], 2012, 531: 55

22 Zuo M, Zhao D G, Teng X Y *et al. Materials & Design*[J], 2013, 47: 857

23 Chang J Y, Kim G H, Moon I G *et al. Scripta Materialia*[J], 1998, 39: 307

24 Li B, Wang H W, Jie J C *et al. Journal of Alloys and Compounds*[J], 2011, 509: 3387

25 Fatih Kilicaslan M, Lee W R, Lee T H *et al. Materials Letters*[J], 2012, 71: 164

26 Tsai Y C, Chou C Y, Lee S L *et al. Journal of Alloys and Compounds*[J], 2009, 487: 157

27 Mao F, Yan G Y, Xuan Z J *et al. Journal of Alloys and Compounds*[J], 2015, 650: 896

28 Sui Y D, Wang Q D, Liu T *et al. Journal of Alloys and Compounds*[J], 2015, 644: 228

29 Qiu H X, Yan H, Hu Z. *Journal of Alloys and Compounds*[J], 2013, 567: 77

30 Yu L N, Liu X F, Ding H M *et al. Journal of Alloys and Compounds*[J], 2007, 429: 119

31 Prasada Rao A K, Das K, Murty B S *et al. Journal of Alloys and Compounds*[J], 2009, 480: 4

32 Liao H C, Zhang M, Wu Q C *et al. Scripta Materialia*[J], 2007, 57: 1121

33 Xu C L, Jiang Q C, Yang Y F *et al. Journal of Alloys and Compounds*[J], 2006, 422: 1

34 Liu W Y, Xiao W L, Xu C *et al. Materials Science and Engineering A*[J], 2017, 693: 93

35 Nadella R, Eskin D G, Du Q *et al. Progress in Materials Science*[J], 2008, 53: 421

36 Li J H, Barrirero J, Engstler M *et al. Metallurgical and Materials Transactions A* [J], 2015, 46: 1300

37 Lu S Z, Hellawell A. *Metallurgical and Materials Transactions A*[J], 1987, 18: 1721

38 Li J H, Hage F, Wiessner M *et al. Scientific Reports*[J], 2015, 5: 13 802

39 Li J H, Suetsugu S, Tsunekawa Y *et al. Metallurgical and Materials Transactions A*[J], 2013, 44: 669

40 Ghomashchi R. *Journal of Alloys and Compounds*[J], 2012, 537: 255

41 Wang T M, Fu H W, Chen Z N e*t al. Journal of Alloys and Compounds*[J], 2012, 511: 45

42 Li Y, Hu B, Gu Q F *et al. Scripta Materialia*[J], 2019, 160: 75

43 Zhou J, Duszczyk J. *Journal of Materials Science*[J], 1990, 25: 4541

44 Li Q L, Xia T D, Lan Y F *et al. Materials Science and Engineering A* [J], 2013, 588: 97

45 Bahrami A, Razaghian A, Emamy M *et al*. *Materials and Design*[J], 2012, 36: 323

Yb 和 Al-Ti-B 复合变质对过共晶 Al-Si 铸造合金组织和性能的影响

李庆林，住玉乾，李进宝，李斌强，刘建军，刘德学，兰睥峰，夏天东

(兰州理工大学 省部共建有色金属先进加工与再利用国家重点实验室， 甘肃 兰州 730050)

摘　要：采用光学显微镜、扫描电子显微镜、电子探针研究了不同比例的稀土 Yb 和 Al-5Ti-B 复合变质剂对过共晶 Al-20Si 合金显微组织与性能的影响。结果表明，Al-20Si 合金中添加质量分数 0.5% Yb 和 0.3% Al-5Ti-1B 复合变质剂使得粗大的多边形状、块状和五瓣星状初生 Si 变质为细小块状，共晶 Si 由粗大的片状或针状结构变质为细小颗粒或者纤维结构，而且粗大的 α-Al 枝晶被细化为等轴枝晶。然而，当 Al-5Ti-B 变质剂含量达到 0.4%时，初生 Si 和共晶 Si 出现粗化现象。力学性能测试结果表明，联合添加 0.5%Yb 和 0.3%Al-5Ti-B 后，合金的抗拉强度和延伸率分别增加了 83.7%和 92.1%。

关键词：过共晶 Al-20Si 合金；初生 Si；共晶 Si；稀土 Yb；Al-5Ti-1B 变质剂；力学性能

作者简介：李庆林，男，1978 年生，博士，副教授，兰州理工大学材料科学与工程学院，甘肃 兰州 730050，电话：0931-2976688，E-mail: liql301@mail.nwpu.edu.cn